BULLETIN OF THE POLISH ACADEMY OF SCIENCES
TECHNICAL SCIENCES, Vol. 68, No. 3, 2020
DOI: 10.24425/bpasts.2020.133375

Influence of the number of turns on the performance of permanent magnet synchronous motor

H. QIU, Y. ZHANG*, C. YANG, and R. YI

School of Electrical and Information Engineering, Zhengzhou University of Light Industry, Zhengzhou, 450002, China

Abstract. The current passed by the stator coil of the permanent magnet synchronous motor (PMSM) provides rotating magnetic field, and the number of turns will directly affect the performance of PMSM. In order to analyze its influence on the PMSM performance, a 3 kW, 1500 r/min PMSM is taken as an example, and the 2D transient electromagnetic field model is established. The correctness of the model is verified by comparing the experimental data and calculated data. Firstly, the finite element method (FEM) is used to calculate the electromagnetic field of the PMSM. The performance parameters of the PMSM are obtained. On this basis, the influence of the number of turns on PMSM performance is quantitatively analyzed, including current, no-load back electromotive force (EMF), overload capacity and torque. In addition, the influence of the number of turns on eddy current loss is further studied, and its variation rule is obtained, and the variation mechanism of eddy current loss is revealed. Finally, the temperature field of the PMSM is analyzed by the coupling method of electromagnetic field and temperature field, and the temperature rise law of PMSM is obtained. The analysis of this paper provides reference and practical value for the optimization design of PMSM.

Key words: eddy current density, losses, PMSM, the number of turns, temperature field.

1. Introduction

The PMSM is widely used in electronic information, mining, communication technology, aerospace, transportation and other fields because of its advantages of simple structure, high efficiency and high power factor [1–3]. The number of turns is an important parameter for the design of the PMSM. The unreasonable design of winding turns will cause larger current in the stator windings. In severe cases, the windings are burnt down. The performance of rotor permanent magnet will also decrease at high temperature. The irreversibly demagnetization of permanent magnet occurs. Therefore, it is of great theoretical significance and practical value to study the influence of winding turns on PMSM performance.

In recent years, many scholars have made relevant studies on the winding turns of motor. In reference [4], it proposes a method for reducing the maximum current of switched reluctance motor by increasing the number of turns. In reference [5], it can be seen that a significant reduction of unbalanced magnetic force is possibly achieved by employing uneven number of turns per coil. In reference [6], it presents a method for selecting the optimum number of turns per phase winding of the switched reluctance motor with a given magnetic configuration and specified operating conditions in terms of the output power and speed. However, in the process of studying the number of turns of the motor, many scholars have not fully studied the influence of the number of turns on PMSM performance, and the influence mechanism of the number of turns on PMSM performance has not been revealed. In addition, based on the electromagnetic field-temperature field coupling method, the sensitivity of temperature field to motor turns is also studied in our manuscript. The range of the number of turns of PMSM to achieve the best performance is determined.

A 3 kW, 1500 r/min PMSM is taken as an example in this paper, based on the two-dimensional FEM, the influences of the number of turns on the magnetic density, torque ripple, output capacity and loss are calculated, and the variation law is obtained. Under the rated operating condition, the eddy current density distribution is studied to reveal the mechanism of eddy current loss. At the same time, the method of electromagnetic field-temperature field coupling is adopted to find the temperature rise law of each part of the PMSM. Based on the above analysis, some useful conclusions will be obtained to improve the performance of PMSM.

2. Motor parameters and models

2.1. Parameters and models. A 3 kW, 1500 r/min PMSM is taken as an example in this paper, as this paper focuses on the influence of the number of turns on the performance of PMSM. The rated speed of the prototype is relatively low and the sheath is not designed to reduce the eddy current loss of the PMSM. According to the structure and parameters of the prototype, the finite element model is established. Table 1 is the basic parameters of PMSM. Figure 1 shows the finite element model of the prototype. The magnetic field lines and magnetic density are also shown in Fig. 1 under no-load operating condition. In the finite element model, the total number of meshes is 10500, which can meet the accuracy of solving.

*e-mail: zhangxiaoyong10056@163.com

Manuscript submitted 2019-11-11, revised 2020-01-19, initially accepted for publication 2020-02-09, published in June 2020

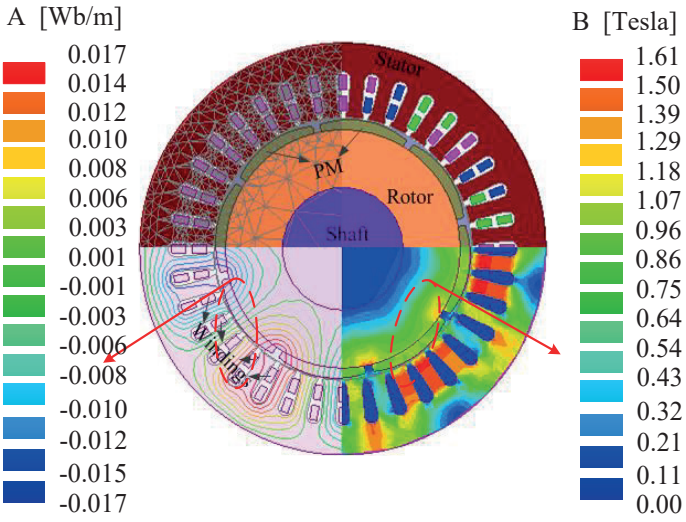

Fig. 1. Finite element model of prototype

Table 1
Prototype parameters

Parameters	Value
Rated power	3 (kW)
Rated speed	1500 (r/min)
Pole number	8
Axial length	72 (mm)
Rotor magnetic circuit structure	Surface-mounted type
Stator outer diameter	168 (mm)
Stator inner diameter	107 (mm)
Slot number	36
Number of parallel branches	1
Winding connection type	Y
Number of turns	26

In order to simplify the analysis of electromagnetic field, the following assumptions are made [7]:

- In the two-dimensional analysis of the PMSM, the end-winding leakage inductance of the PMSM is ignored.
- Ignoring the influence of PMSM displacement current, the parallel plane field perpendicular to the motor shaft is adopted to analyze the electromagnetic field of the PMSM.
- The influences of PMSM temperature on material conductivity and magnetic conductivity are ignored.

The calculation formula of two-dimensional electromagnetic field is shown in (1) [8]:

$$\begin{cases} \Omega: \dfrac{\partial}{\partial x}\left(\dfrac{1}{\mu}\dfrac{\partial A_z}{\partial x}\right)+\dfrac{\partial}{\partial y}\left(\dfrac{1}{\mu}\dfrac{\partial A_z}{\partial y}\right)=-J_z+\sigma\dfrac{dA_z}{dt} \end{cases} \quad (1)$$

where Ω is the calculation region, A_Z and J_Z are magnetic vector potential and the source current density in the Z-axial component, respectively, σ is conductivity, μ is permeability, and t is time.

The stator slot area is constant. When the number of turns is changed, the wire diameter should be changed so as to keep the copper filling factor constant. There is research premise to the article.

2.2. Experimental test and data comparison. In order to verify the accuracy of the model, the prototype is tested by experimental platform. The experimental platform includes Magtrol dynamometer machine, HIOKI PW6001 power analyzer, industrial condensing unit, DSP data acquisition system and other experimental equipment. The experimental platform of the prototype is shown in Fig. 2. Under different operating conditions, the experimental data of torque, no-load back EMF and current are obtained. The experimental data is compared with the calculated data, as shown in Table 2.

Table 2
Comparison between experimental data and calculated data

Power		2 kW	3 kW	3.5 kW
Calculated results	Average torque	12.6 (N•m)	19.2 (N•m)	22.1 (N•m)
	Armature current	5.9 (A)	8.9 (A)	10.1 (A)
	No-load back EMF	151 (V)		
Test data	Average torque	12.7 (N•m)	19.1 (N•m)	22.3 (N•m)
	Armature current	5.8 (A)	8.7 (A)	10.09 (A)
	No-load back EMF	150 (V)		
Change rate	Average torque	1.7%	2.3%	0.1%
	Armature current	0.8%	0.5%	0.9%
	No-load back EMF	0.7%		

Fig. 2. Prototype test platform

It can be seen from Table 2 that the errors are within 5%. The calculated results are in good agreement with the experimental data under different power. The accuracy of the model is verified.

3. The theoretical analysis

$$R_1 = \rho_{75} \frac{2N_1 L_{av}}{A_1 a_1} \tag{2}$$

$$X_m = 4f\mu_0 \frac{m}{\pi} \frac{m(N_1 K_{dp1})^2}{p} l_{ef} \frac{\tau}{\delta_{ef}} \tag{3}$$

where R_1 is phase resistance of stator, ρ_{75} is the resistivity of copper at 75°C, N_1 is the number turns, L_{av} is the average length of half turns, A_1 is conductor cross-section, a_1 is number of parallel branch, X_m is the end leakage reactance of stator, K_{dp1} is winding factor, f is frequency, μ_0 is permeability of vacuum, p is the number of pole-pairs, δ_{ef} is effective air gap length, l_{ef} is armature calculation length, τ is polar distance.

When the number of turns is different, the resistance and reactance of the stator winding are also different. It can be seen from the resistance calculation equation (2) that the resistance of the stator winding is proportional to the number of turns. It can be seen from the reactance calculation equation (3) that when other parameters are unchanged, the reactance of the stator winding is proportional to the square of the number of turns.

The resistance and end leakage reactance of stator winding should be calculated when the number of turns is different. Based on different resistances and end leakage reactance of stator winding, the influence of the number of turns on PMSM performance is quantitatively analyzed.

3.1. The influence of the number of turns on the performance. The no-load back EMF is one of the important parameters, and it can judge the performance of the PMSM [9, 10]. The no-load back EMF need to be accurately calculated. In the design of PMSM, when the number of turns is unreasonable, the stator windings will be damaged by the excessive current. In addition, it will cause larger torque ripple, which will cause greater vibration and noise in the process of PMSM operation. Therefore, this section focuses on the influence of the number of turns on overload capacity, output capacity, armature current and no-load back EMF.

In this paper, the torque ripple formula (4) is used to measure the torque ripple [11]:

$$T_{ripple} = \left| \frac{T_{max} - T_{min}}{2 \times T_{avg}} \right| \times 100\% \tag{4}$$

T_{max} is the maximum torque in a cycle. T_{min} is the minimum torque in a cycle and T_{avg} is the output capacity in a cycle.

When the number of turns is 20, 22, 24, 26, 28, 30 and 32 respectively, the performance parameters of PMSM are shown in Fig. 3. From Fig. 3, it can be seen that the output capacity increases by 24.6%, when the number of turns is reduced by 2. When the number of turns increases by 2, the overload capacity increased by 8%.

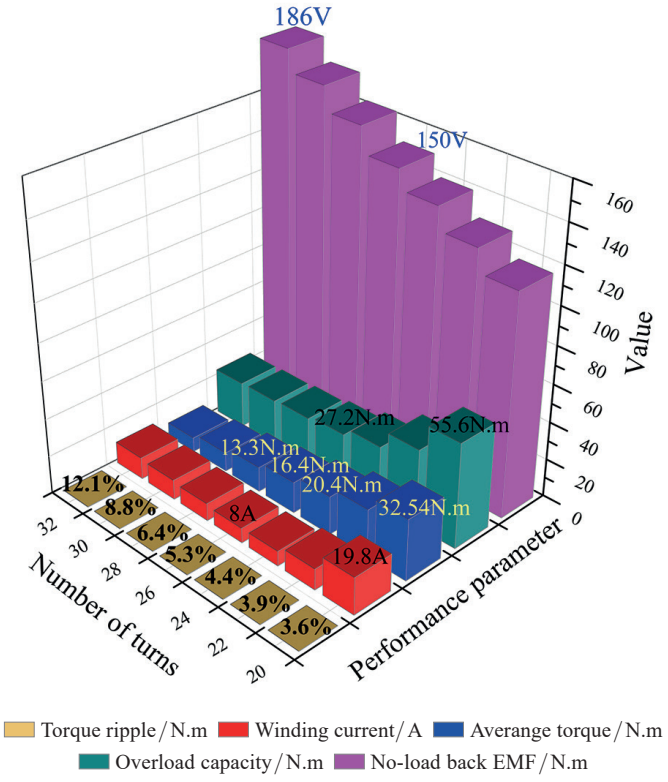

Fig. 3. The influence of the number of turns on PMSM performance

With the increase of winding turns, the torque ripple obviously increases. In addition, with the increase of winding turns, the output capacity and the overload capacity decrease sharply. With the increase of the winding turns, the armature current shows a V shape curve, and the current is the lowest at 26 turns. The no-load back EMF shows an exponentially increasing trend with the increase of the number of turns.

Figure 4 shows the variation curve of the number of turns with the power factor at different power angles. From Fig. 4, it can be seen that increasing the number of turns can improve the power factor, and combined loss analysis, the efficiency shows a V-shaped variation, which is the highest at 26 turns. Combining with Fig. 3, excessive turns will also bring the adverse influence on the PMSM, such as excessive current and the reduction of overload capacity.

It can be known from the above analysis that when the number of turns of PMSM is different, there is a huge difference in the torque ripple, winding current, output capability, no-load back EMF and overload capacity of the motor. Therefore, in the design of the PMSM, it is necessary to synthesize various performance parameters and choose the best winding turns.

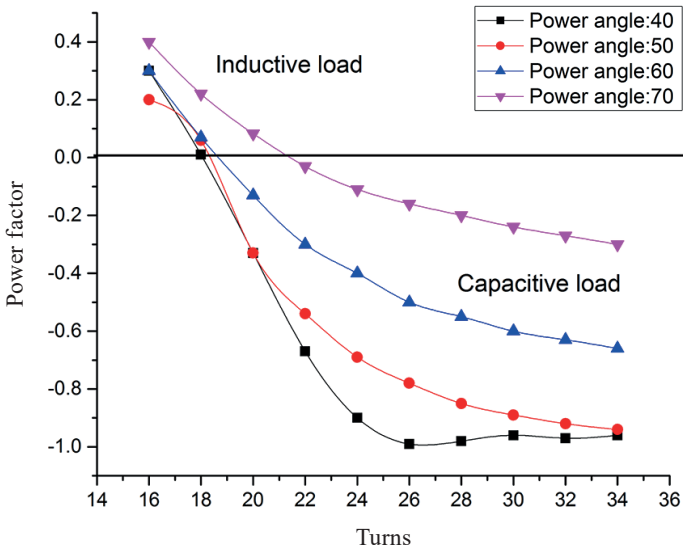

Fig. 4. The curves of power factor

4. The influence of the number of turns on the loss of PMSM

Loss is the main index to measure the efficiency of PMSM. The variation of winding turns can cause great changes of current and magnetic field, which causes the variation of PMSM loss. Therefore, it is very valuable to study the influence of the number of turns on PMSM loss. According to the mechanism of core loss, the core loss of PMSM can be divided into the hysteresis loss and the eddy current loss. The eddy current loss can be divided into classical eddy current loss and abnormal eddy current loss. The calculation formula of core loss is the formula (5) [12]:

$$P_{\mathrm{Fe}} = P_h + P_c + P_e = \\ = 190 \times fB^2 + 0.822 \times f^2 B^2 \tag{5}$$

where P_{Fe} is the core loss, P_h is the hysteresis loss, P_c is the classical eddy current loss, P_e is the excessive loss, f is the frequency, *and* B is the flux density.

It is obtained from the formula (5) that the core loss of the PMSM is related to the frequency and the magnetic density. Based on the FEM, the influences of the number of turns on the stator core loss and eddy current loss of the PMSM are studied, and the variation law of the winding turns on the PMSM loss is obtained.

4.1. The analysis of stator core loss. Because the stator core is made of silicon steel sheet with high resistivity and good magnetic conductivity, the eddy current losses in the stator core are greatly reduced. The main component of the stator core loss is the hysteresis loss. Because the magnetic field strength is closely related to the hysteresis loss [13], the magnetic field strength is affected by the winding turns, and the hysteresis loss can also change. The magnetic field distributions under different winding turns are shown in Fig. 5.

It can be seen from the Fig. 5 that when the number of turns is different, the distribution of magnetic flux lines is obviously different. When the number of turns of the PMSM is 26, the magnetic induction is 1.65 *Wb/m*, and the distribution of magnetic field is symmetric. When the number of turns is 20 and 32, its magnetic induction intensity is 1.77 *Wb/m* and 1.60 *Wb/m* respectively. The magnetic induction decreases with the increase of winding turns.

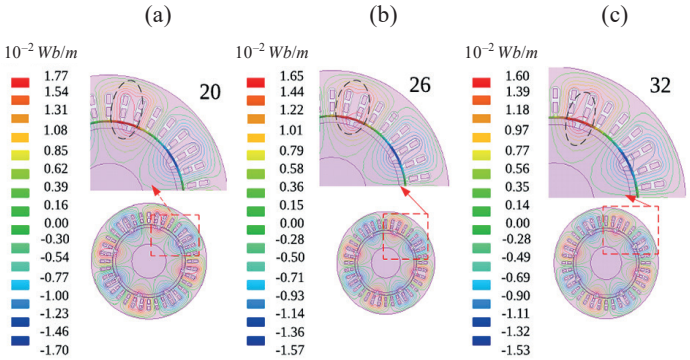

Fig. 5. The magnetic force line distribution

In order to observe the saturation of the PMSM magnetic field more clearly, the variation of the magnetic field distribution with different winding turns is shown in Fig. 6.

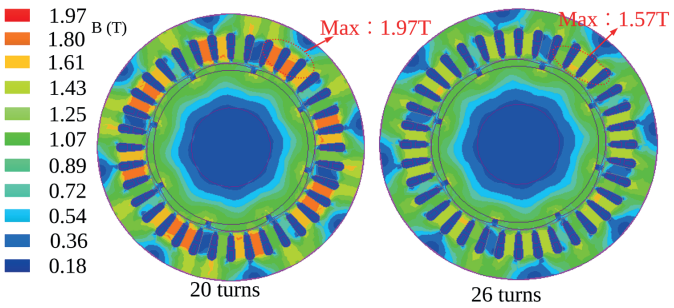

Fig. 6. The motor magnetic field distribution under different turns

When the number of turns is 26, the maximum magnetic density is 1.57 T, and the magnetic field distribution is suitable. The magnetic field is damaged when the number of turns is reduced, and the magnetic saturation is serious. The magnetic density in local region is even more than 2 T. Because the hysteresis loss is affected by the magnetic field intensity, the hysteresis loss gradually increases with the decrease of the number of turns. Table 3 shows the stator core loss at the different number of turns.

The number of turns of the prototype is 26, and the stator core loss is 40.6 W. With the reduction of the number of turns, the stator core loss increases gradually. The stator core loss is

Table 3
The stator core loss under different winding turns

Turns	Core loss (W)	Change rate (%)
20	64.2	58
22	54.2	33.5
24	46.5	14.5
26	40.6	0
28	36.0	−11.3
30	32.3	−20.4
32	29.3	−27.8

64.2 W when the number of turns is 20. The stator core loss increased by 58% compared with that the stator core loss of the prototype.

4.2. Eddy current loss. The induced EMF and the eddy current in the conductors are induced by the alternating magnetic flux, and then the eddy current loss is formed [14]. The eddy current loss is mainly formed in the permanent magnet and the sleeve. The increase of eddy current loss will cause the increase of the temperature of permanent magnets, and the performance of permanent magnets will decrease. In very severe cases, the permanent magnet will have irreversible loss of excitation, which will cause great harm to the normal operation of the PMSM. Therefore, this section focuses on the influence of changing the number of turns on the eddy current loss. The rotor eddy current density distributions under different conditions are shown in Fig. 7.

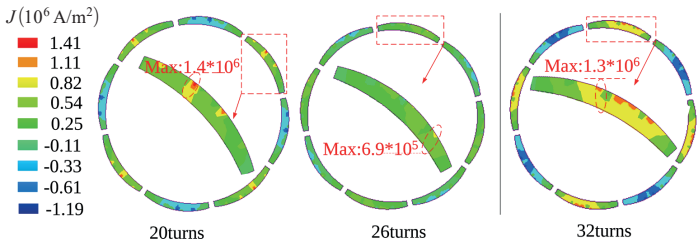

Fig. 7. The rotor eddy current density distribution

During the calculation, the rotor eddy current losses in the rotor surface are calculated by the "(6)" in a cycle [15]:

$$P_e = \frac{1}{T_e}\int_{T_e}\sum_{i=1}^{k} J_e^2 \Delta_e \sigma_r^{-1} l_t \, dt \tag{6}$$

where Pe is the rotor eddy current losses (in W), J_e is the current density in each element $\left(\text{in A/m}^2\right)$, Δ_e is the element area $\left(\text{in m}^2\right)$, l_t is the rotor axial length (in meters), σ_r is the conductivity of the eddy current zone (in S/m), T_e is the time vary period of eddy current density in each element.

When the number of turns is 26, the rotor eddy current density distributes suitably in the circumferential direction, and the maximum value is 6.9×10^5 A/m^2. With the increase or decrease of the number of turns, the eddy current density and the eddy current loss both are increased. The change of the rotor eddy current loss with the change of the turns is shown in Fig. 8.

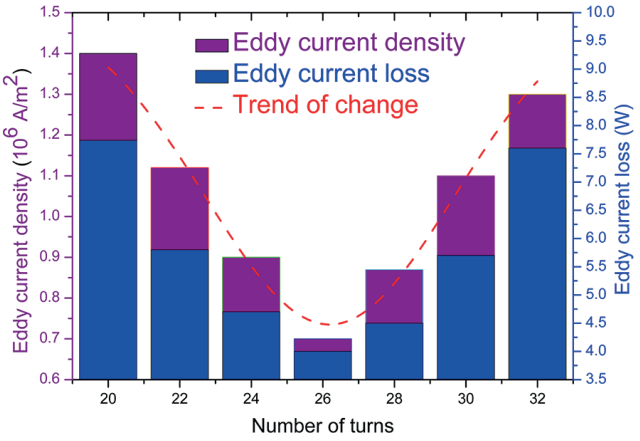

Fig. 8. Eddy current loss and eddy current density

When the number of turns is 26, the rotor eddy current loss is 4 W. Combined with Fig. 3, it can be seen that with the deepening of the winding turns increasing or decreasing, the influence of winding turns on the current is obvious. Because of the influence of the pulse magnetic field generated by the current on the eddy current density, the eddy current density changes obviously under winding turns increasing or decreasing.

The eddy current loss and the eddy current density shows V shape, and show the lowest value at 26 turns. When the number of turns is increased or reduced, the distribution of eddy current density is obviously different. When the number of turns is 20, the peak value of the rotor eddy current density is 1.4×10^6 A/m^2, and increases by 2.03 times compared with when the number of turns is 26. The rotor eddy current loss increases to 8 W, and increases by 2 times compared with that the number of turns is 26.

5. The temperature field distributions

The motor stator windings are separated by the insulating material. The insulation level under different working conditions and environments is different. When the operating temperature exceeds the maximum tolerance temperature of the permanent magnet, the demagnetization phenomenon of the permanent magnet will occur. Changing of the number of turns has great influence on the motor temperature distribution. The temperature rise is a major factor that threatens the magnetic property of the permanent magnet, the winding insulation, stable operation and the service life of the PMSM.

The loss of motor is the heat source of motor temperature. In order to study the influence of the number of turns on the temperature field of the PMSM, the main loss of the motor can be obtained by the finite element electromagnetic field calculation, as shown in Table 4.

Table 4
The main loss of the motor under different winding turns

Turns	Core loss (W)	Eddy current loss (W)	Copper loss (W)
20	64.2	7.7	419.5
22	54.2	5.8	158.0
24	46.5	4.7	96.5
26	40.6	4.0	115.3
28	36.0	4.5	177.8
30	32.3	5.7	266.6
32	29.3	7.5	359.8

It can be seen from Table 4 that with the increase of the number of turns, the core loss gradually decreases, and the eddy current loss and the copper loss shows V shape. The eddy current loss shows the lowest value at 26 turns and the copper loss shows the lowest value at 24 turns. In addition, the copper loss and core loss are the main heat sources for motor temperature.

Based on the analysis results of the PMSM loss in the previous section, the temperature field-electromagnetic field coupling method is used to analyze the temperature field distribution of the PMSM under the different number of turns. The variation law of temperature of each part of the PMSM is obtained.

5.1. Temperature field model. In order to simplify the analysis and calculation of the temperature field, the following assumptions are proposed [16].

- The heat exchange between the stator and rotor only through the air gap.
- The PMSM is continuous along axial direction, and the axial temperature gradient is zero.
- The influence of the temperature generated by the PMSM during operation on the thermal conductivity is ignored.
- The temperature gradient of the core in the axial direction is zero, and there is no heat transfer in the axial direction of the motor and only the radial heat transfer is considered. The 3D temperature field model is simplified to 2D temperature field model for analysis.

Based on above assumptions, the 2-D model could be established adopting the FEM, as shown in Fig. 9. Heat transfer equation can be expressed as the equation (7) [17].

$$\begin{cases} \dfrac{\partial}{\partial x}\left(\lambda_x \dfrac{\partial T}{\partial x}\right) + \dfrac{\partial}{\partial y}\left(\lambda_y \dfrac{\partial T}{\partial y}\right) = -q_v \\ -\lambda_x \dfrac{\partial T}{\partial x}\Big|\Gamma = \alpha\left(T - T_f\right) \end{cases} \tag{7}$$

where T is the body temperature (in °C), l is thermal conductivity coefficient [in W/(m*°C)], q_V is the heat generation density $\left(\text{in W/m}^2\right)$, the stator outer surface is air natural convection heat dissipation, the third boundary condition is given as G (the stator outer circle boundary), n is unit normal vector on the shell surface, a is heat transfer coefficient, T_f is temperature of the circumstance (in °C).

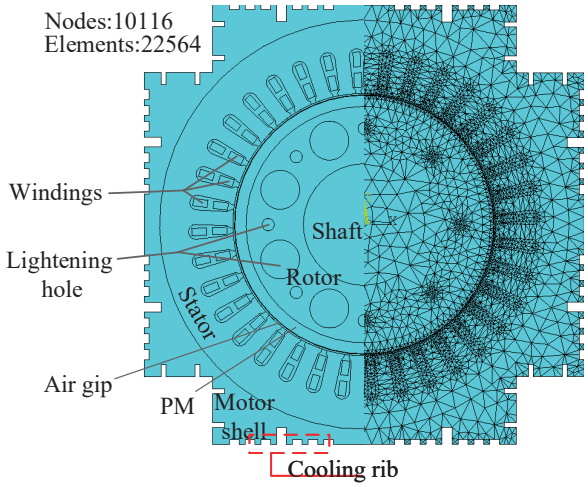

Fig. 9. The motor temperature field model

5.2. The temperature field analysis results. In order to analyze the influence of the number of turns on the PMSM temperature field, the temperature distribution of each component is analyzed based on the FEM. The environmental temperature of PMSM running is 25°C. The temperature distributions under different conditions are shown in Fig. 10.

When the number of turns is 26, the temperature distribution characteristics are as follows:

- The windings temperature is the highest, and the value is 130.4°C. The temperatures of the inner windings and outer windings are different, and the maximum temperature difference appears in the dense distribution of the cooling rib.
- The rotor eddy current loss is only 4 W. Because the thermal conductivity of the air gap is poor, the heat generated in the rotor could not be dissipated in time. The permanent magnet temperature is 120.7°C and the shell temperature is 118.7°C.

The overall temperature of the PMSM distribution increases significantly, when the number of turns is difference. When the number of turns is 20, the maximum temperature of the

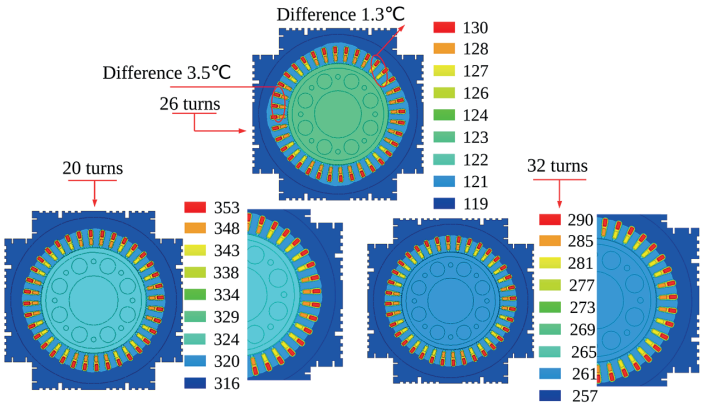

Fig. 10. The temperature field distributions under different turns

winging is 355.5°C, which increases 3 times compared with that the number of turns is 26. The maximum temperature of the permanent magnet increases by 2.7 times, and it is obviously affected by the winding temperature rise. When the number of turns is 32, the maximum temperature of the winging is 290°C, which increases by 2.2 times compared with that the number of turns is 26. The maximum temperature of the permanent magnet increases 2 times.

When the number of turns of the motor is different, the core loss and copper loss of the motor change greatly. They are the main losses in the motor. Therefore, they are also the main heat source of the motor.

The important factors affecting the variation degree of the number of turns are the maximum operating temperature of the permanent magnet and the winding insulation level. When the motor increases the overload capacity by reducing the number of turns, the above two factors should be fully considered. This will ensure the safe and stable operation of the motor.

With the deepening of the number of turns increases or decreases, the PMSM loss of each part increases gradually, so does the temperature. The maximum insulation class of the PMSM can withstand temperatures of 180°C. The winding insulation and the permanent magnet magnetic property will be severely affected, and the PMSM will eventually burn out.

6. Conclusions

In this paper, the following conclusions are obtained by studying the influence of the number of turns on the PMSM performance:

- With the decrease of the number of turns, the magnetic density shows non-linear growth trend, which leads to significant increase of magnetic density in each part. The magnetic density in the local region is even more than 2 T. With the decrease of the number of turns, the stator core loss of the PMSM increases exponentially. When the number of turns is reduced by 23%, the core loss increases by 58%.
- With the increase or decrease of the number of turns, the variation trend of eddy current density and eddy current loss is synchronized, and shows a V shape curve. When the number of turns of PMSM is varied, the eddy current density and eddy current loss change significantly. When the number of turns is 26, the eddy current loss is the smallest, reaching 4 W. When the number of turns is reduced by 23%, the eddy current loss increases by 2 times.
- When the number of turns is slightly increased or decreased, the temperature of each part of the PMSM changes sharply. When the number of turns is reduced by 23%, the maximum temperature of the winding increases to 355°C, increasing by nearly 3 times, and the maximum temperature of the permanent magnets to 327°C, increasing by nearly 2.6 times. With the deepening of changing the number of turns, the PMSM loss increases gradually, and the temperature of each part increases gradually, and the PMSM will eventually burn out.
- With the increase of the number of turns, torque ripple and no-load back EMF obviously increase, and the output capacity and maximum torque decrease sharply. The armature current presents V shape with the increase of the number of turns, and the current is the smallest at 26 turns, which is consistent with the variation law of the eddy current loss.

Acknowledgements. This work was supported in part by the National Natural Science Foundation of China under Grant 51507156, in part by the University Key Scientific Research Programs of Henan province under Grant 17A470005, in part by the Key R & D and Promotion Projects of Henan Province under Grant 182102310033, in part by the Doctoral Program of Zhengzhou University of Light Industry under Grant 2014BSJJ042.

References

[1] K. Urbanski, "A new sensorless speed control structure for PMSM using reference model", *Bull. Pol. Ac.: Tech.* 65(4), 489–496 (2017).

[2] T. Tarczewski, "High-performance PMSM servo-drive with constrained state feedback position controller", *Bull. Pol. Ac.: Tech.* 66(1), 49–58 (2018).

[3] K. Urbanski, "Unscented and extended Kalman filters study for sensorless control of PM synchronous motors with load torque estimation", *Bull. Pol. Ac.: Tech.* 61(4), 489–496 (2013).

[4] Chiba, M. Takeno, N. Hoshi, M. Takemoto, S. Ogasawara, and M.A. Rahman, "Consideration of Number of Series Turns in Switched-Reluctance Traction Motor Competitive to HEV IPMSM," *IEEE Trans. Ind. Appl.* 481(6), 2333–2340 (2012).

[5] S.M. Al-Habshi, M.L. M. Jamil, M.N. Othman, A. Jidin, K.A. Karim, and Z.Z. Zolkapli, "Influence of number of turns per coil in fractional-slot PM brushless machines," *2014 IEEE Conference on Energy Conversion (CENCON)*, Johor Bahru, 2014, pp. 146–151.

[6] J. Corda, "Search for optimum number of turns of switched reluctance motor," V *IEEE International Power Electronics Congress Technical Proceedings*, *CIEP 96*, *Cuernavaca*, 1996, pp. 241–245.

[7] C.X. Yang and Y. Zhang, "Influence of Output Voltage Harmonic of Inverter on Loss and Temperature Field of Permanent Magnet Synchronous Motor." *IEEE Trans. Magn.* 55(6), 82016056,(2019).

[8] A. Łebkowski, "Design, Analysis of the Location and Materials of Neodymium Magnets on the Torque and Power of In-Wheel External Rotor PMSM for Electric Vehicles", *Energies* 11(9), 1–23 (2018).

[9] H. Zhan, Z.Q. Zhu, and M. Odavic, "Nonparametric Sensorless Drive Method for Open-Winding PMSM Based on Zero-Sequence Back EMF With Circulating Current Suppression," *IEEE Trans. Power Electron.* 32(5), 3808–3817 (2017).

[10] X. Sun, "Design and analysis of interior composite-rotor bearingless permanent magnet synchronous motors with two layer permanent magnets", *Bull. Pol. Ac.: Tech.* 65(6), 833–843 (2017).

[11] V.S. Nagarajan, "Geometrical sensitivity analysis based on design optimization and multiphysics analysis of PM assisted synchronous reluctance motor", *Bull. Pol. Ac.: Tech.* 67(1), 49–58 (2019).

[12] B.K. Su, X. Sun, and L. Chen, "Thermal modeling and analysis of bearingless permanent magnet synchronous motors," *Int. J. Appl. Electromagn. Mech.* 56(1), 115–130 (2018).

[13] H.B. Qiu, W.F. Yu, and B.X. Tang, "Research on the Influence of Inter-turn Short Circuit Fault on the Temperature Field of Permanent Magnet Synchronous Motor," *J. Electr. Eng. Technol.* 12(4), 1566–1574 (2017).

[14] S. Chaithongsuk, N. Takorabet, and S. Kreuawan, "Reduction of Eddy-Current Losses in Fractional-Slot Concentrated-Winding Synchronous PM Motors," *IEEE Trans. Magn.* 51(3), 1–4 (2015).

[15] J. Han, W. Li, L. Wang, X. Zhou, X. Zhang, and Y. Li, "Calculation and Analysis of the Surface Heat-Transfer Coefficient and Temperature Fields on the Three-Dimensional Complex End Windings of a Large Turbogenerator," *IEEE Trans. Ind. Electron.* 61(10), 5222–5231 (2014).

[16] Y. Xia, Y. Xu, M. Ai, and J. Liu, "Temperature Calculation of an Induction Motor in the Starting Process," *IEEE Trans. Appl. Supercond.* 29(2), 1–4 (2019).

[17] J.X. Li, C.M. Zhang, and L.L. Li. "Calculation and Experimental Study on Temperature Rise of a High OverLoad Tubular Permanent Magnet Linear Motor", *IEEE Trans. Plasma Sci.* 41(5),1182–1187 (2013).